DOI: 10.71762/1ecq-0d33

Research Paper

Design and Simulation of a Trapezoidal Die for use in the Constrained Groove Pressing Process and Investigation of the Effect of the Process Die Displacement on the Strain of Stainless Steel 316 Plate

Mohammad Hassan Raoufian [1], Mohammad Hydari [1], Ahmad Afsari[2*]

[1]Department of Mechanical Engineering, Aligudarz Branch, Islamic Azad University, Aligudarz, Iran

[2]Full Professor, Department of Mechanical Engineering, Shiraz Branch, Islamic Azad University, Shiraz, Iran

*Email of Corresponding Author: Ah.afsari1338@iau.ac.ir & Dr.afsari1@yahoo.com

Received: August 17, 2025; Revised: October 01, 2025 Accepted: October 12, 2025

Abstract

Materials with superior mechanical properties have a wide range of applications in various industries such as aerospace, automotive, medical, petroleum, and petrochemical. In this regard, although stainless steel 316 has desirable properties such as resistance to rust, corrosion, and creep, its performance still needs improvement. Therefore, by subjecting a steel part to shear deformation by the constrained groove pressing (CGP) process, it is possible to improve its grain structure and mechanical properties. By changing the upper die displacement during processing, the strain applied to a three mm-thick piece can be altered. In this study, an attempt has been made to investigate the effect of varying die displacement on the strain changes in a 316 steel plate in ABAQUS. The results indicate that as die displacement increases, the part's strain increases. If the amount of displacement increases so much that the distance between the two dies becomes less than the thickness of the steel plate, the strain increases, and the cross-sectional area of the steel plate changes. While in displacements where the distance between the two sides of the die is greater than the thickness of the steel plate, the maximum strain does not occur at a distance equal to the thickness of the steel plate, but the maximum strain is achieved before reaching the thickness of the steel plate. In displacements of 12.58 to 12.88 mm, the strain rates are close to each other, but the maximum strain does not occur at the displacement of 12.88 mm; instead, the maximum strain is created in the first step at the displacement of 12.58 mm, and in the third step, at the displacement of 12.68 mm. At displacements lower than 12.88 mm in the first and third steps of the process, the shape of the part changes from trapezoidal to curved.

Keywords

Simulation, Trapezoidal Die, Constrained Groove Press (CGP), Displacement, Stainless Steel 316

1. Introduction

In industry, materials with superior mechanical properties are desirable. In this regard, stainless steel 316 is used in various applications, such as the marine, food and pharmaceutical, medical equipment (surgical instruments and implants), chemical, automotive, and aerospace industries, due to its high

resistance to corrosion and heat. Due to its unique chemical composition and molybdenum content, stainless steel 316 offers an excellent balance of corrosion and heat resistance. These properties make it ideal for use in corrosive environments and high temperatures, especially in sensitive industries such as marine, chemical, and medical. Also, the high flexibility in welding and machining, combined with its ability to withstand a variety of conditions, makes it a superior choice for demanding, challenging applications compared to other stainless steel grades such as 304 and 430. The SPD[1] has become an effective tool for manufacturing sheets with superior properties and is attractive for a wide range of industrial applications [1-2]. The process of metal forming without removing material has a long history and is called metal forming. Severe plastic deformation is a method that allows the structure and mechanical properties of materials to be significantly modified by applying severe mechanical loads. The SPD process is particularly effective for improving the mechanical strength and ductility of metallic materials. Severe plastic deformation in metallic materials can be achieved using various methods such as ARB[2], ECAP[3], CGP[4], and RCS[5]. These processes produce significant material deformations, resulting in an excellent structure. The RCS process involves subjecting an alloy sheet to repeated cycles of plastic deformation and straightening. During the deformation step, the sheet undergoes a series of undulations induced by specific mechanical forces. These grooves help to form the sheet [3-6]. In the CGP process, the material is subjected to repeated shear deformation by the inverse stress between the grooved and flat dies. To prevent any dimensional changes due to the process, the die is constructed in such a way that the material is confined along its length and must be subjected to repeated passes, each pass consisting of four steps, two steps consisting of alternating grooving operations and 180° rotation with two stages of flattening operations, the schematic of which is shown in (Figure 1) [7-9]. At the end of each pass, the entire material is subjected to an effective plastic strain. Distinctive advantages of CGP over other processes include no dimensional change in the processed plate, considerable stress applied in a single pass, ease of material production and fabrication, and a simple experimental setup. Improvement of mechanical properties through CGP has been achieved in a wide range of metallic materials with different crystal structures, including low-carbon steel, aluminum, and titanium. Along with the dislocation change, other grain boundary effects, such as grain boundary diffusion and sliding, occur, leading to increased toughness [10-16].

[1] Severe plastic deformation
[2] Accumulative roll bonding
[3] Equal channel angular pressing
[4] Constrained groove pressing
[5] Repetitive corrugation and straightening

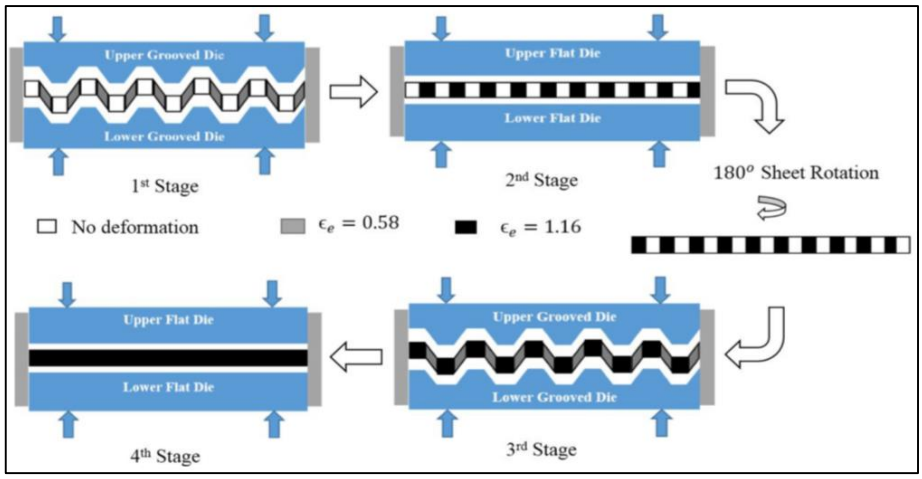

Figure 1. Schematic of the Constrained Groove Pressing (CGP) process [7]

During the CSP[6], the sheet is severely deformed and undergoes strain. According to the CGP method, the applied strain should be homogeneous throughout the surface. However, in practical conditions, strain heterogeneity is observed in the sample sheet. The amount of strain heterogeneity in the sheets is greater than the corresponding amount of the average strain applied to the sheets at different stages. The tensile and compressive strains, which lead to a higher imposed strain, are also distributed heterogeneously. To increase grain refinement, CGP with conventional dies at a 45° groove angle induces shear deformation, and repeated pressings lead to the development of a fine-grain structure. However, the use of conventional dies leads to local strain in the sample and severe surface effects. Therefore, more micro-cracks are formed [16-18].

Zimina et al. [19] investigated the microstructure and microhardness of an ultrafine-grained material prepared by confined groove pressing of AZ31 cast magnesium strips. Microstructural observations showed a significant reduction in grain size from 200 to 20μm after CGP. Furthermore, the observed inhomogeneity in microhardness across the cross-section suggests that the CGP method is a good process for grain refinement of magnesium alloys. An improvement in micro-hardness accompanies grain refinement to the point where there is almost no reduction in sample thickness (less than 10%), and the inhomogeneity in microstructure and micro-hardness along the cross-section of the sample can be minimized after further cycles CGP process. Nagarajua et al. [20] investigated the thermal stability of the microstructure of 6061 aluminum alloy produced by the CGP method. The sample processed by CGP exhibited enhanced mechanical properties, attributed to an UFG[7] and microstructure refinement [1]. The results showed that the tensile strength, micro-hardness, and thermal stability of the CGP-processed sample were higher than those of the untreated samples. The good thermal stability of CGP samples is probably due to the presence of triple grain boundaries and the blockage of grain boundary motion. The number of CGP passes had a significant effect on the micro-hardness and ultimate tensile strength properties. Mozafari et al. [21] evaluated the abrasion behavior of UFG alloys produced by the SPD method and compared it with coarse-grain alloy. For this purpose, weight reduction, wear resistance, friction coefficient, and morphology of worn surfaces

[6] Constrained Studded Pressing
[7] Ultrafine-grain structure

were investigated. The results showed that using the CGP process and forming the UFG structure significantly increases strength, hardness, and abrasion resistance. In a study [7], the rate of hardness change during the CGP process, a plastic deformation technique applied to metals, was investigated. They concluded by modeling and simulating the CGP process and comparing numerical analysis results with experimental results, finding that strength increases with increasing the number of passes. Nazari et al. [22] studied the effect of heat treatment and Stress relieving on mechanical properties, microstructure, and residual stresses by the severe plastic deformation method, known as the CGP process. For this purpose, the CGP process was performed on a 3 mm thick commercial pure copper sheet. The hardness, strength, homogeneity, microstructure, and residual stresses were evaluated before and after the stress-relieving and annealing heat treatment. The hardness and homogeneity were investigated at the surface and throughout the thickness, and the strength was determined in both the groove and transverse groove directions. Also, the microstructure along the thickness of the CGP specimens was studied. The results show that as the number of CGP passes increases, hardness, strength, and homogeneity increase, while the average grain size and residual stress decrease. Kumar and Vedrtnam [23] investigated the effects of process-induced residual stresses CGP on the hardness, tensile strength, and grain size of aluminum and copper. They reported improvements in tensile strength and hardness after each pass, due to reduced grain size.

Dhiliban et al [18] studied the CGP process numerically and experimentally to analyze the strain distribution by changing the die profile to a sinusoidal shape. They concluded that AA2014 specimens pressed using a sinusoidal die profile had lower strain non-homogeneity than those pressed using a conventional die with a 45 ° groove angle. It was observed that the surface texture improved, and a total of 40 passes were possible with a sinusoidal mold, compared to 4 with a conventional 45° groove-angle die. Hosseini et al. [24] investigated the effect of the process reset angle on the microstructure and mechanical properties of pure copper sheets processed by the constrained studded pressing CSP[1] process experimentally and numerically. The results show that the first pass CSP reduced the crystal size in both die sets to nanometer levels and increased the dislocation density in the samples significantly. The 60° dies caused greater strain, more severe dislocation accumulation, and consequently more severe dynamic recovery in the copper sample than the 30° dies, resulting in the ultimate strength of the samples from the 60° dies decreasing more than that of the 30° dies. It has also been shown that a pass CSP with a reset angle of 30° can achieve a higher ultimate tensile strength in pure copper sheets than the groove press or the conventional CGP method.

One of the challenges of the CGP process is the non-uniform strain distribution, which is due to the relationship between the applied strain and the material's mechanical properties, leading to a non-uniform distribution of mechanical properties within the material structure. This undesirable effect can limit the use of deformed samples for some applications. Increasing the uniformity of strain distribution is the goal of this research, for which it is necessary to investigate the change in the distance between the two dies to eliminate the non-uniformity of the strain distribution, so that by creating strain uniformity by the CGP process, it is possible to improve the mechanical properties. In this regard, the CGP process simulation was performed in ABAQUS to investigate the strain at different die displacements in austenitic stainless steel 316 and to determine the effect of the CGP process die displacement on the applied strain, as well as how different displacements distort the part.

In addition, the effects of die displacement on the cross-section and improvement of mechanical properties have been investigated.
Austenitic stainless steel 316 has different names in different standards; some examples are given in Table 1.

Table1. Austenitic stainless steel 316 has different names in different standards

stainless steel	Japanese standard	Swedish Standard	European standard		British Standard		
316	JIS	SS Swedish	Name	NO.	EN	BS	USN NO.
	SUS316	2347	X5CrNiMo17-12-2	1.4401	58H	316S31	S31600

Different elements make up the composition of 316 stainless steel. Table 2 lists the elements that make up 316 stainless steel.

Table 2. Different elements make up the composition of 316 stainless steel

stainless steel	N	C	Mn	S	P	Si	Mo	Ni	Cr
316	0.10	0.03	2.0	0.03	0.045	0.75	3.0	12.0	18.0

Stainless steel 316 has different properties, such as physical and mechanical properties. The physical properties of this metal are listed in Table 3. The properties needed for this research include mechanical properties, as detailed in Table 4 [25-31].

Table3. Physical and mechanical properties of stainless steel 316

stainless steel	Specific heat capacity J/kg.K	Thermal conductivity W/m.K	Electrical resistance nΩ.m	Elastic modulus GPa	Density Kg/m3
316	500	16.3	740	193	7880

Table 4. Mechanical properties of Stainless Steel316

stainless steel	Hardness HB	Hardness HRB	Elongation	Yield strength MPa	Tensile strength MPa
316	217	95	40%	220	520

By knowing these properties, the CGP process can be simulated in ABAQUS software on stainless steel 316 and the effect of the amount of die displacement in the CGP process on the strain applied to the part can be examined.

2. The CGP Process

To increase the uniformity of the strain distribution, a trapezoidal die (Figure 2) has been used to improve the uniformity of the plastic strain applied to the plate. It should be noted that the uniformity of the mechanical structure is related to the uniformity of the applied strain; in other words, the greater the uniformity of the plastic strain in the deformed sample, the greater the isotropy of the deformed sample.

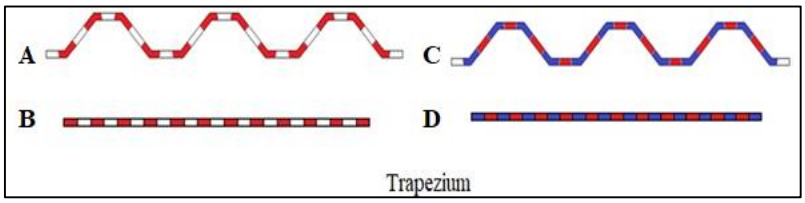

Figure 2. Applying shear strain to the plate by trapezoidal die: The four stages of the trapezoidal die are shown in order from letters A to D

In the constrained groove pressing process, a complete pass consists of four consecutive steps, two steps performed by the grooved die and two steps performed by the flat die. In the first step of each pass, a 3 mm thick sheet of metal is placed between two grooved dies with a width of 30 mm, a height of 40 mm, and a groove height of 15.88 mm. The upper die can move only vertically. While the bottom die is fully restrained. After the upper die approaches the lower die, the parts of the sheet located in the inclined areas of the dies are subjected to shear stress, as shown in Figure 2A, while deformation does not occur in the flat areas of the sheet. In the second stage (Figure 2B), the sheet metal is compressed by a pair of simple flat dies, which causes the parts of the sheet that have been deformed in the first stage to undergo reverse shear deformation to flatten the sheet. After the second stage and before the third and fourth stages of the process, the plate is rotated 180 degrees about the die's vertical axis. Also, 180 degrees about its longitudinal axis so that the areas deformed in the first stage are located in the flat areas of the grooved die, and the previously unformed areas are located on the inclined areas of the die.

3. The CGP Process simulation

3.1 The CGP Process schematic

Figure 3 shows the CGP Process schematic and the sequence of operations for pressing a constrained groove with a rectangular cross-section with a trapezoidal-shaped die.

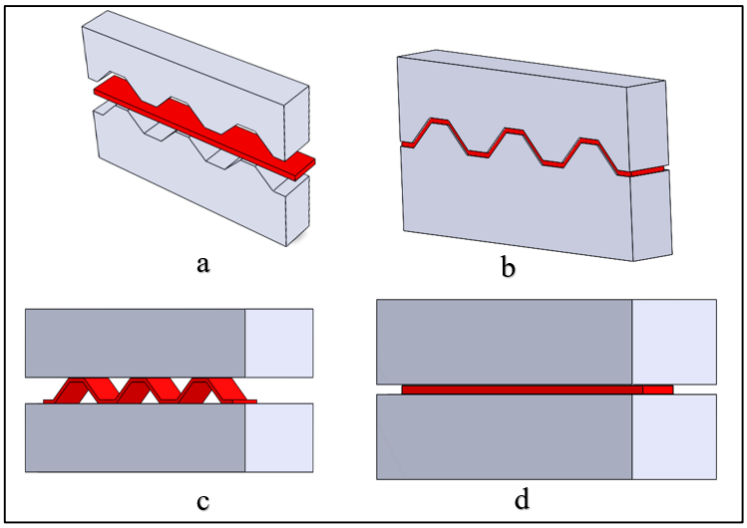

Figure 3. Schematic of the CGP process using a trapezoidal die: a) Trapezoidal die and plate before pressing, b) Plate and trapezoidal die after pressing, c) Straightening die and shaped plate before straightening, and d) Straightening die and straightened plate

3.2 (CGP) Process simulation

The CGP process was simulated, and a trapezoidal die was performed using ABAQUS software on a stainless steel 316 plate. In this model, the steel plate has a thickness of 3 mm and is fully passed through the CGP process using a trapezoidal die. A schematic of the upper and lower dies, including their dimensions and angles, is provided in Figure 4. The dimensions are specified in millimeters, and the die angle is 45 degrees.

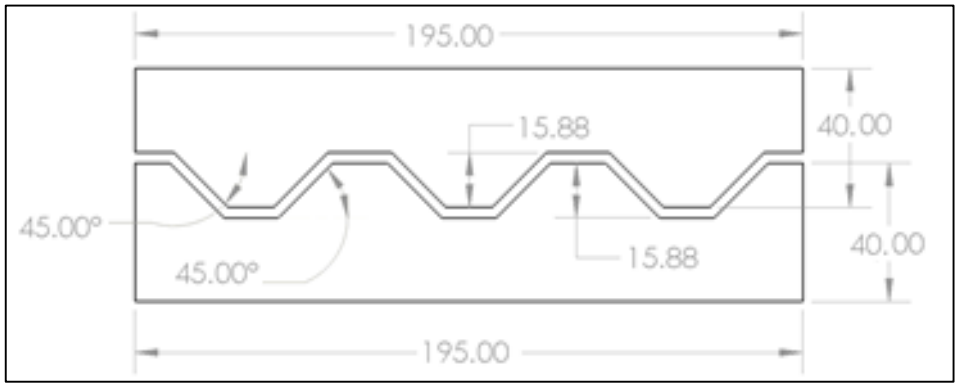

Figure 4. A schematic of the upper die and lower die and their dimensions

To simulate the CGP process in ABAQUS, it is necessary to define the plastic strain equations correctly. The governing Equation is presented below. The basic plastic strain equation for the CGP process in ABAQUS uses the power-law model, as shown in Equations (1) and (2). [32].

$$\sigma = k(\varepsilon_{Pl})^n \quad (1)$$

$$\varepsilon_{pl} = (\frac{\sigma}{K})^{\frac{1}{n}} \quad (2)$$

σ: Plastic stress

k : Strength Coefficient

ε_{Pl}: Plastic strain
n : Strain Hardening Exponent

The material and properties of the stainless steel plate and the forming and straightening dies are given in Table 5. In this simulation, the coefficient of friction (μ) is assumed to be 0.15 [22].

Table 5. The material and properties of the stainless steel plate, the forming and straightening dies and degree of freedom in process

	Material	Elastic modulus (GPa)	Poisson's Ratio	degree of freedom
Upper Die	AISI 4140	210	0.3	1
Bottom Die	AISI 4140	210	0.3	0
Plate	stainless steel 316	200	0.3	0

At each stage of the analysis, the movement of the bottom die is restricted in all directions, while the upper die is allowed to move only vertically on the plate. The amount of die displacement during the deformation process in the trapezoidal die is 12.88 mm. To investigate the effects of die displacement on the strain applied to the plate, the amount of 12.88 mm was changed to observe the effects of displacement. The strain was investigated at displacements of 12.08, 12.18, 12.28, 12.38, 12.48, 12.58, 12.68, 12.78, 12.88, 12.98, and 13.08mm. Figure 5 shows the CGP process simulation in ABAQUS software.

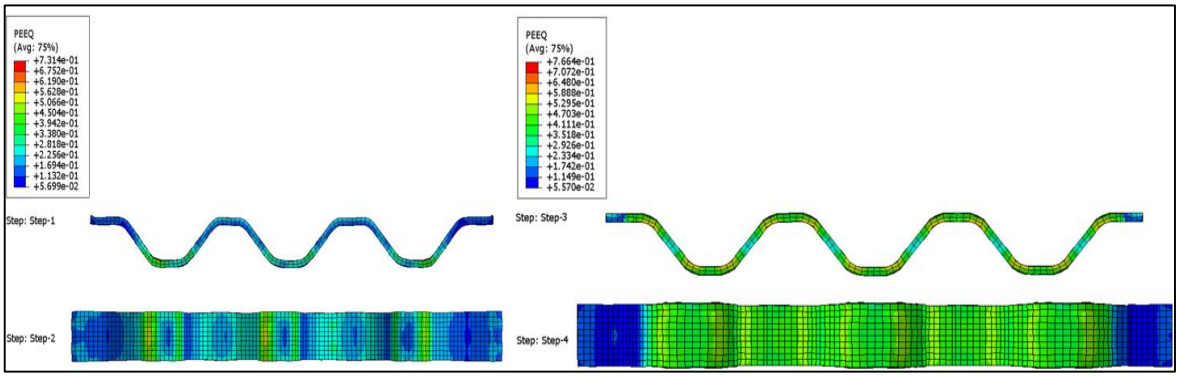

Figure 5. Strain changes in the plate during the trapezoidal die simulation operation

3.3 Mesh convergence CGP process simulation

In addition to the primary research topic, the design of a finite element method study often requires appropriate model configurations, good meshing, and a specific simulated scenario [32]. Finite element analysis (FEA), also called the finite element method (FEM), is a method for numerical solution of field problems. In mechanical engineering, one seeks the distribution of displacement, stress, pressure, or load, for example. Individual finite elements (FE) mesh the studied region in a finite number of small pieces, which are represented by a system of algebraic equations to be solved for unknowns at their nodes. These sets of equations depend on the mesh geometry, size, and

resolution method. Thus, the structure field quantity is only approximated and accumulates the approximations, but can be optimized by selecting appropriate parameters. Unfortunately, this accuracy often has a cost: the central processing unit CPU time, also called solver time. In engineering and research fields, a compromise must be made between accuracy and calculation time. Therefore, the main goal is to find a balance between the accuracy of the results and the computational cost [33-34]. Therefore, Table 6 lists the approximate seed size and number of elements. Figure 6 shows the mesh convergence graph over a 10-second time interval. As shown, an element count of 2200 can balance accuracy and problem-solving time.

Table 6. The approximate seed size and number of elements

Approximate seed size	0.5	0.75	1.0	1.5	2	2.5	3.0	3.5	4
Number of elements	105660	31644	13200	3800	2200	704	511	378	275

Figure 6, shows an image of the meshed upper and lower die and the metal plate. The element shape is hex.

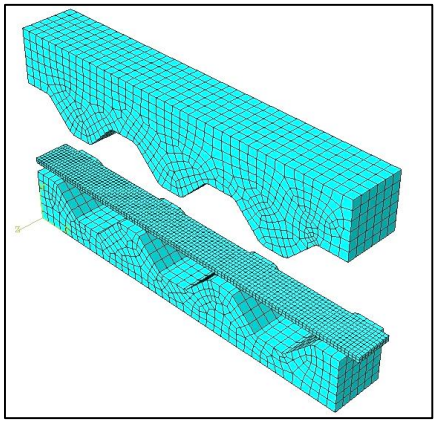

Figure 6. The meshed upper and lower molds and plate

Figure 7 shows the mesh convergence diagram for the CGP process. Finally, the analysis of this process is of the dynamic- explicit type and the number of elements used is 2200.

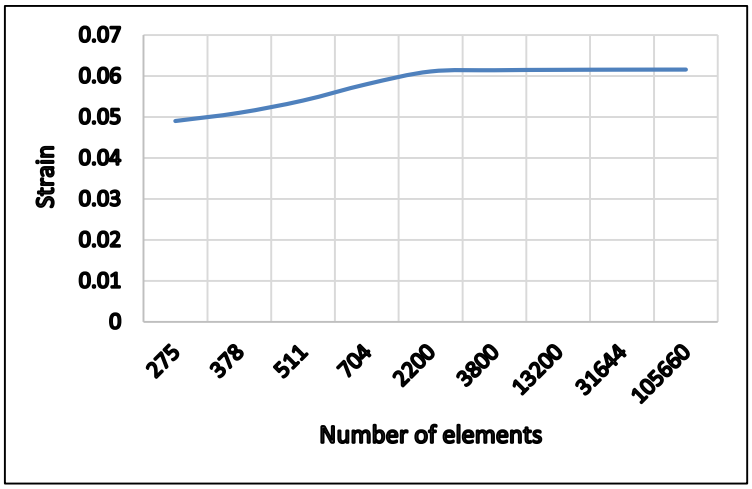

Figure 7. Mesh convergence diagram

4. Results and discussion

Some results were obtained by examining the displacement of the upper die. In the simulation results, it was observed that the strain rate decreased at displacements less than 12.48 mm in the first stage of the process. While the strain-time graphs are very close to each other from displacements of 12.48 mm to 12.88 mm, for displacements greater than 12.98 mm, the strain rate increases. Figure 8 shows the simulation of a trapezoidal die in the 15-second time interval of the first stage of the CGP process with a displacement of 12.68 mm in ABAQUS software.

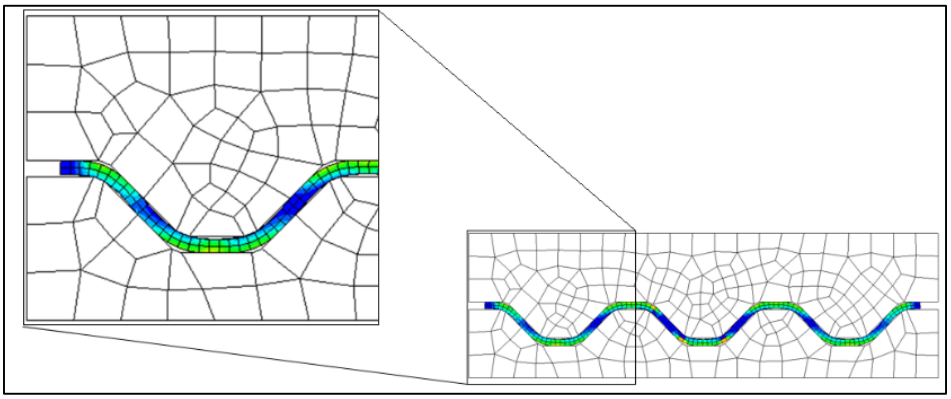

Figure 8. Simulation of a trapezoidal die in the first stage of the process (CGP) with a displacement of 12.68 mm in ABAQUS software, during a 15-second time interval

At displacements above 12.98 mm, the strain increases, but on the other hand, as seen in Figure 9, the thickness of the part decreases, which indicates a decrease in the thickness of the cross-sectional area of the plate.

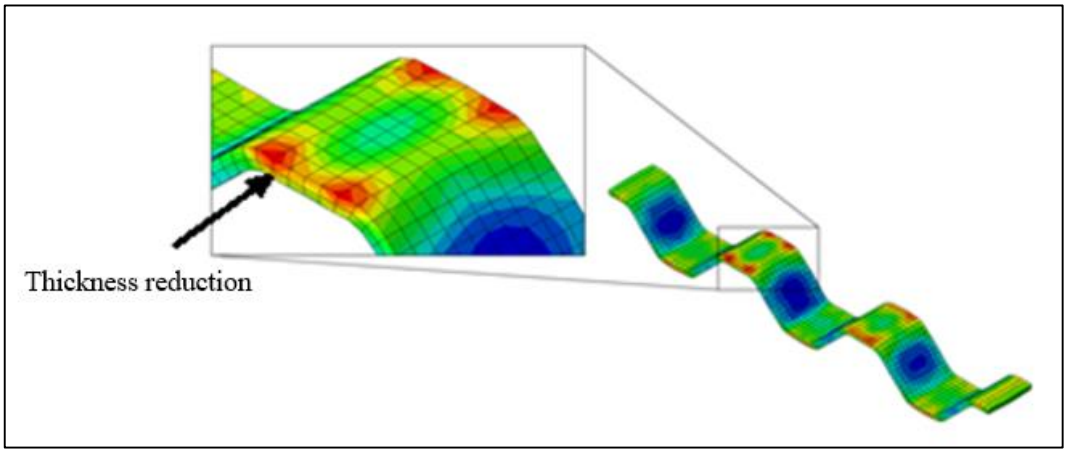

Figure 9. Simulation of a trapezoidal mold in a time interval of 15 seconds in ABAQUS software, the CGP process with displacement of 13.08 mm and reduction of plate thickness

According to Figure 10, the strain should decrease for displacements less than 12.48 mm; this decrease in strain, in turn, reduces the shear strain. On the other hand, the decrease in strain indicates that a smaller amount of the plate is affected by the shear strain. Figure 10 shows the strain versus time diagram at displacements of 12.48 to 12.88 mm in the first stage of the process.

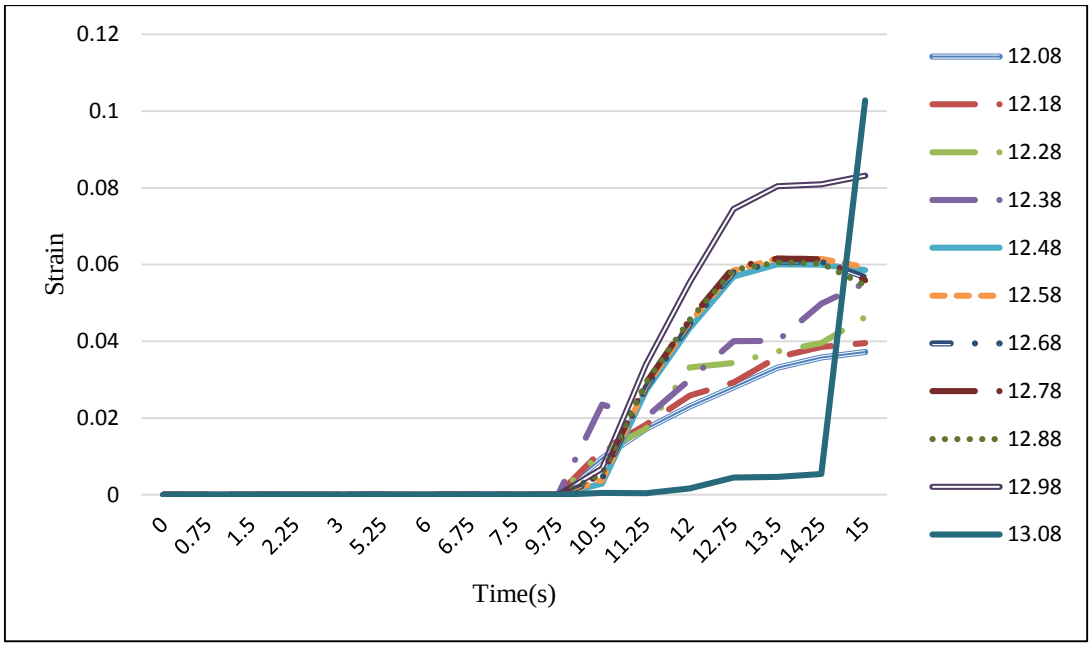

Figure 10. Strain change diagram in terms of upper die displacement in a trapezoidal die simulation over a 15-second time period in the first stage of the CGP process

As shown, the diagrams are very similar, with the highest strain occurring at displacements of 12.48-12.88 mm in the first stage (Figure 11). As shown in Figure 12, the maximum effective strain of the first stage of the process CGP is in the range of 0.060055-0.061564. And the maximum strain occurs at a displacement of 12.58 mm.

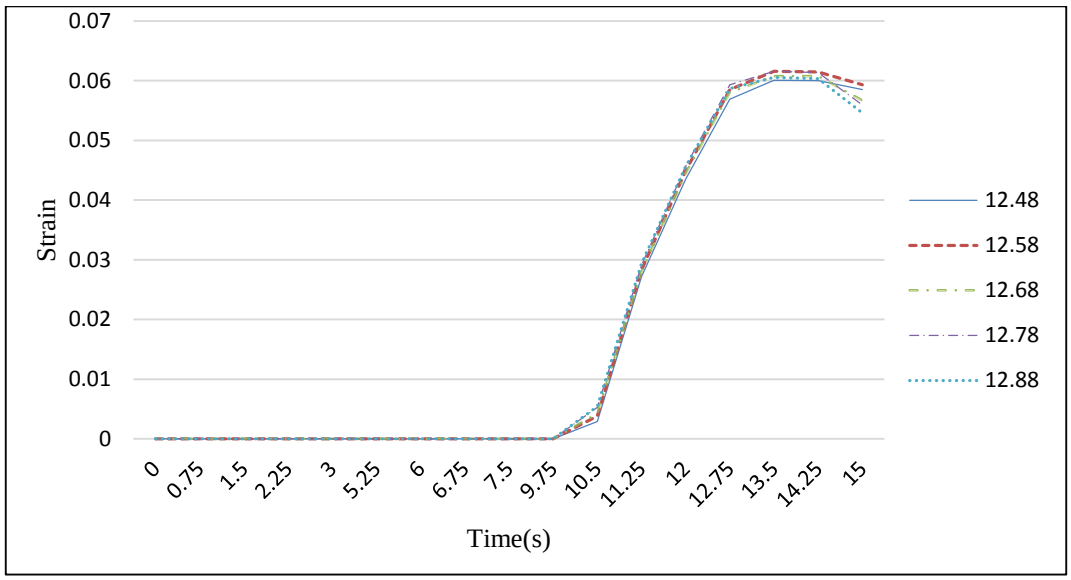

Figure 11. Diagram of strain changes in terms of upper die displacement (12.48-12.88mm) in a trapezoidal die simulation over a 15-second time period in the first stage of the CGP process

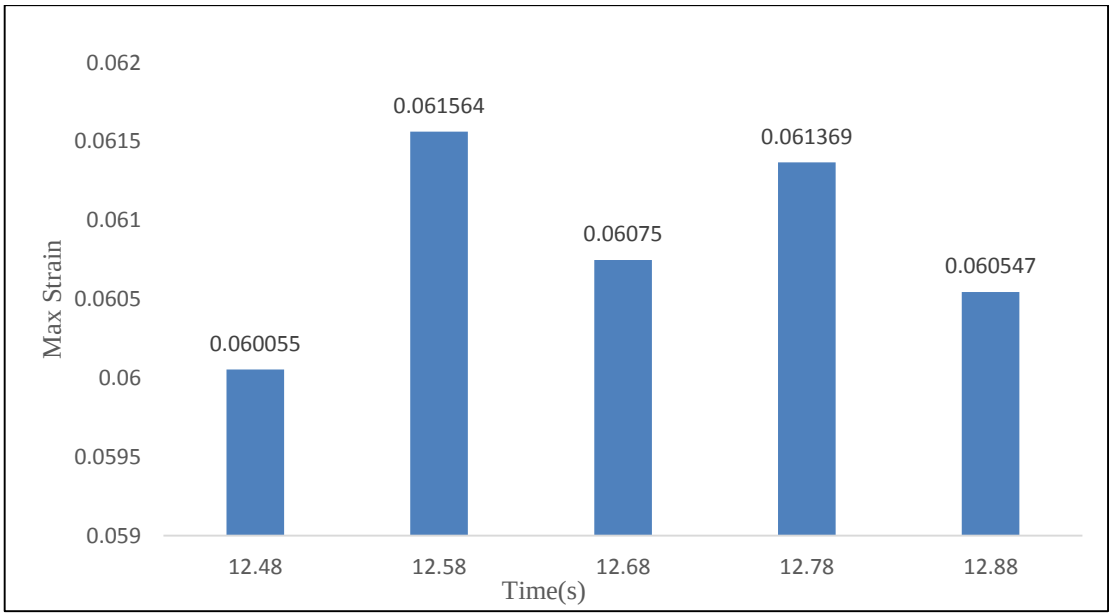

Figure 12. Maximum strain diagram at displacements of 12.48, 12.58, 12.68, 12.78 and 12.88 mm, upper mold in trapezoidal mold simulation, time interval 15 seconds, first stage of (CGP) process

In the third stage of the process, similar to the first stage, the results from the simulator (Figure 13) show that at displacements less than 12.48 mm, the strain rate decreases, and on the other hand, at displacements greater than 12.98 mm, the strain rate increases, while the strain-time curve from displacement 12.48 mm to 12.88 mm is very close to each other.

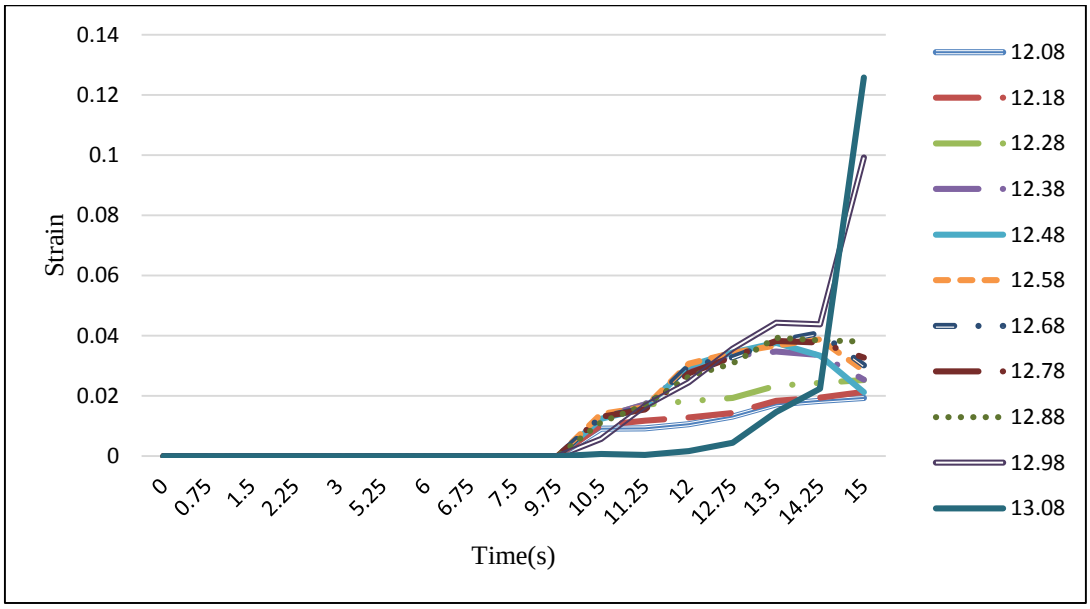

Figure 13. Strain change diagram in terms of upper mold displacement in a trapezoidal die simulation over a 15-second time period in the third stage of the CGP process

As can be seen, the diagrams are very close to each other. The highest strain at displacements of 12.48 to 12.88 mm (Figure 14).

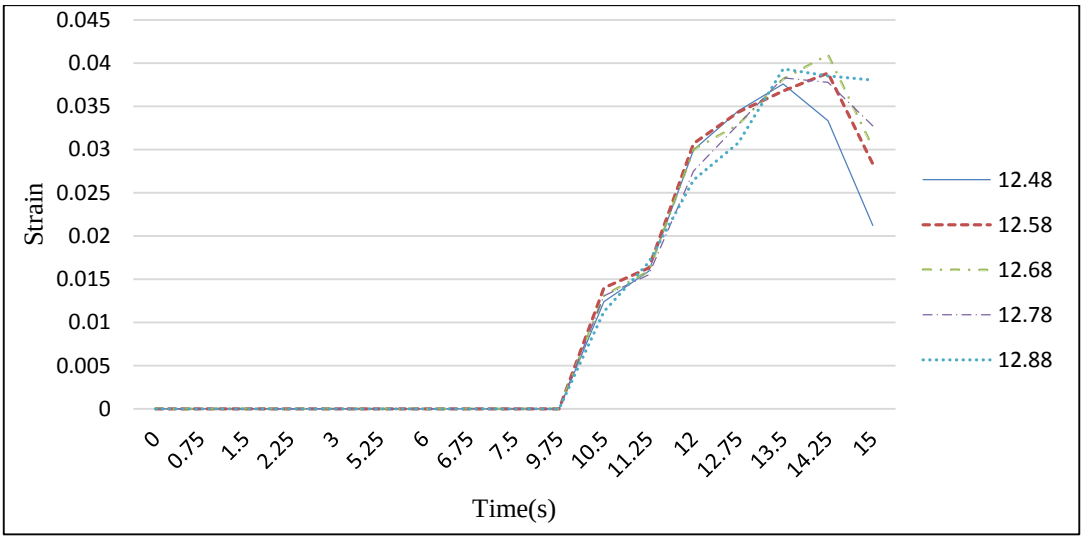

Figure 14. Strain change graph based on upper mold displacement in a trapezoidal die simulation over a 15-second time period in the third stage of the (CGP) process

Figure 15 shows that the maximum effective strain of the third stage of the CGP process is in the range of 0.035241 to 0.040946. And the maximum strain occurs at a displacement of 12.68 mm. As shown in Figure 16, the thickness change at the end of the CGP process is given. The thickness reduction causes a change in the cross-sectional area of the plate. A displacement greater than 12.98 mm causes a thickness reduction of more than 10%. In the CGP process, the amount of thickness reduction should be below 10%.

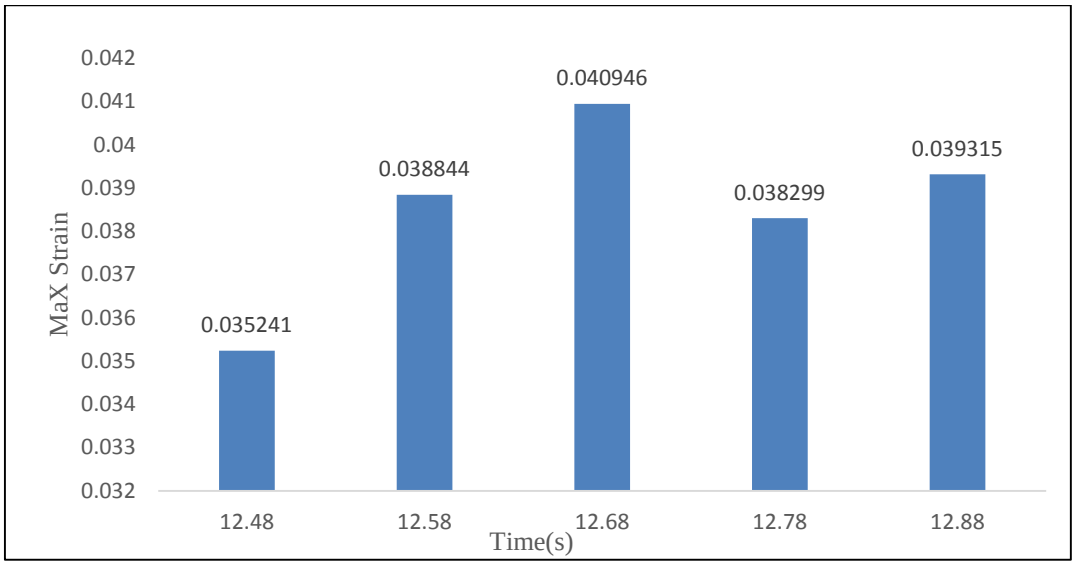

Figure 15. Maximum strain diagram at displacements of 12.48, 12.58, 12.68, 12.78 and 12.88 mm, upper mold in trapezoidal die simulation in a time interval of 15 seconds in the third stage of the CGP process

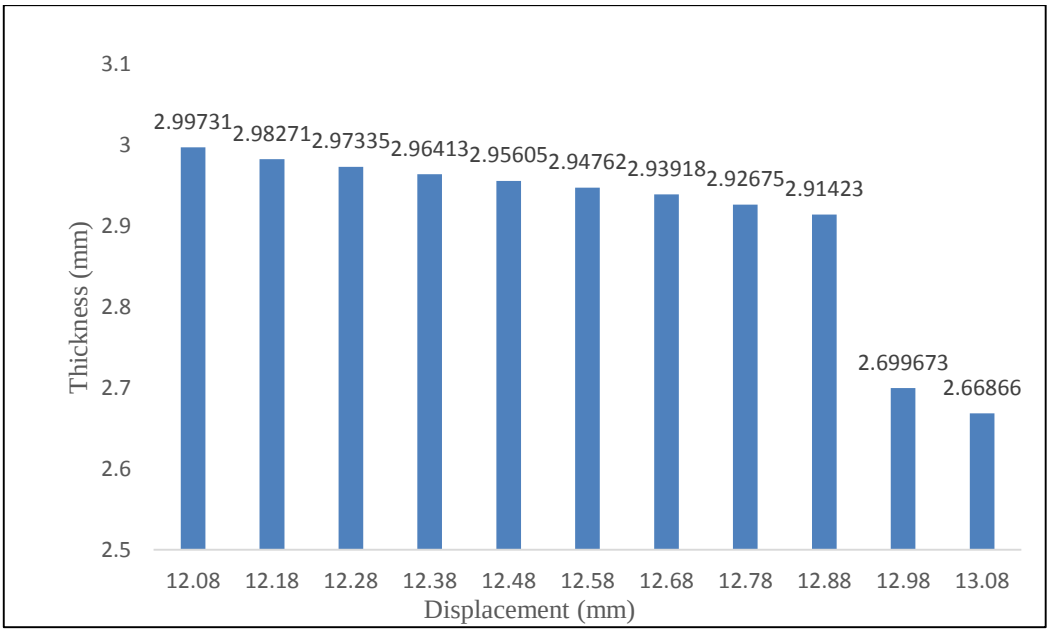

Figure 16. Graph of plate thickness changes depending on displacement in the CGP process

Strains can be classified into different types, with axial and shear strains among the most important. Therefore, in the ABAQUS software, the strain that it presents as the final and output strain is the sum of all strains. In the die displacement range of 12.48 to 12.88, the dominant strain is shear, which is desirable for this process. According to Figure 9, in the CGP process, at a displacement of 13.08mm, the elements colored red should be blue or pale green. This means that less strain is applied to these elements. As a result, the process runs properly until 14.25 seconds. Still, from 14.25 seconds onward, as the upper die descends, the elements are compressed, the part thickness decreases sharply, and finally, a sudden shift is observed in the strain-time diagram.

The pure strain of a process is the strain applied to the part due to the form created by the process. Many factors affect the strain applied to the plate, making it difficult to determine the net strain of the process. Finding the pure strain is significant and helps observe more clearly and investigate the effects of the process on the plate. One parameter that can misrepresent study results is the amount of upper die displacement in the limited-groove pressing process. By simulating the CGP process with the trapezoidal die in the ABAQUS software, by examining the amount of strain in different displacements of the upper die in the first and third stages of the CGP process applied to a 316 stainless steel plate, it was determined that the strain is affected by the displacement of the upper die. If the upper die displacement is low, the strain applied to the plate is reduced, which in turn reduces the pure strain and prevents the grain-refinement mechanism from functioning properly, thereby preventing the CGP process from achieving its goal. If the displacement of the upper die is too large and the distance between the upper and lower dies is less than the thickness of the plate, the strain applied to the part will increase. However, two points are essential: first, not all the strain applied to the part is pure process strain, and second, the plate will be distorted, and this distortion will cause the thickness of the part to decrease by more than 10%, contradicting the process assumption that the thickness of the plate remains constant. In between, there is a range of upper die displacement where the process strain is introduced into the plate. It should be noted that the highest pure strain does not

occur in the displacement where the distance between the upper and lower dies is equal to the thickness, but rather the highest strain occurs at the distance that is the greatest from the thickness of the plate. Applying the maximum strain means that a larger area of the part is involved in shear strain, which means increasing the uniformity and homogeneity of the strain distribution in the plate. Ultimately, the shape of the process die grooves CGP is trapezoidal, but at the maximum strain, i.e., displacement before reaching the thickness of the plate, the shape imposed on the plate is not a trapezoidal shape with a definite angle, but a shape with angles inclined to a curve, and the shape of the part tends from trapezoidal to semicircular.

5. Conclusion

In the CGP process, the amount of die displacement affects the strain applied to the plate; therefore, by examining different displacements in ABAQUS, the following results were obtained.

1. Displacement less than 12.48 mm reduces the strain rate and the effective strain, and does not cause significant changes in the plate's structure.
2. As mold displacement increases, the effective strain increases. So that in the range of 12.58 to 12.88 mm, the strain change tables are almost close to each other, and from displacement 12.98 mm and above, the strain rate increases sharply.
3. At displacements of 12.98 mm or greater, this increase in strain is due to the plate's stretching and compression. As a result, not all of this strain is due to the CGP process, and it is evident that this strain is not the desired strain for the process.
4. At displacements of 12.98 mm or more, an excessive increase in strain causes a reduction of more than 10% of the thickness, which is also not desirable.
5. At a displacement of 13.08mm, the process runs properly until 14.25 seconds. Still, from 14.25 seconds onward, as the upper die descends, the elements are compressed, the part thickness decreases sharply, and finally, a sudden shift is observed in the strain-time diagram.
6. At displacements 12.58 to 12.88 mm, the strain rates are close to each other, but the highest strain does not occur at displacement 12.88 mm. The highest strain occurs in the first step at a displacement of 12.58 mm and in the third step at 12.68 mm.
7. At displacements lower than 12.88 mm during the first and third steps, the shape of the plate transitions from trapezoidal to semicircular.

7. References

[1] Gupta, A.K., Tejveer, S.M. and Singh, S.K. 2016. Constrained Groove Pressing for Sheet Metal Processing: A Review. Progress in Materials Science. doi:10.1016/j.pm atsci.2016.09.008.

[2] Rastitalab, A., Khajehpour, S., Afsari, A., Heidari, S. and Dehghani, J. 2021. An Investigation of Using RCS-processed Intramedullary Stainless Steel 316L Nail in the Treatment of Diaphyseal Bone Fractures. Journal of Modern Processes in Manufacturing and Production. 10:3. dor: 20.1001.1.27170314.2021.10.3.8.1.

[3] Rastitalab, A., Khajehpour, S., Afsari, A., Heidari, S. and Dehghani, J. 2021. Mechanical Stability of RCSed and ECAPed Intramedullary 316L Stainless Steel Nails in the Treatment of Diaphyseal

Bone Fractures. Journal of Modern Processes in Manufacturing and Production.10:4. dor: 20.1001.1.27170314.2021.10.4.3.8.

[4] Elyasia, M., Talebi-Ghadikolaeeb, H., Ahmadi Khatirc, F. and Modanloo, V. 2024. Numerical and experimental study of energy absorption in multilayer tubes manufactured through spinning forming process under quasi-static axial loading. Alexandria Engineering Journal. 106:571–581. doi:10.1016/j.aej.2024.08.038.

[5] De la Trinidad, C.A., Elizalde, S., Cabrera, J.M., Figueroa, I.A. and Gonzalez, G. 2024. Texture study of an AA5083 processed by Repetitive Corrugati on and strengthening. Journal of Materials Research and Technology.30:2690–2697. doi:10.1016/j.jmrt.2024.04.014.

[6] Heidari, S. and Afsari, A. 2021. Study of Mechanical Properties of 7075 Aluminum Alloy Due to Particle Size Reduction due to Constrained Groove Pressing CGP Process Journal of Modern Processes in Manufacturing and Production.10:1. dor: 20.1001.1.27170314.2021 .10 .1.1.0.

[7] Kumar, S., Hariharan, K., Kumar, R. and Paul, S.K. 2019. Accounting Bauschinger effect in the numerical simulation of constrained groove pressing process. Journal of Manufacturing Processes. 38:49–62. doi:10.1016/j.jmapro. 2018.12.013.

[8] Shin, DH., Park, JJ., Kim, YS. and Park, KT. 2002. Constrained groove pressing and its application to grain refinement of aluminum. Mater Sci Eng A.328(1):98–103.

[9] Khodabakhshi, F., Kazeminezhad, M. and Kokabi, A. 2010. Constrained groove pressing of low carbon steel: nano-structure and mechanical properties. Mater Sci Eng A. 527(16):4043–9.

[10] Kumar, S.S. and Raghu, T. 2014. Structural and mechanical behavior of severe plastically deformed high purity aluminium sheets processed by constrained groove pressing technique. Mater Des. 57 :114–20.

[11] Khorrami, MS., Kazeminezhad, M. and Kokabi, A. 2015. Thermal stability of aluminum after friction stir processing with SiC nanoparticles. Materials Des. 80:41–50.

[12] Kumar, G., Niranjan, G.G. and Uday, C. 2011. Grain refinement in commercial purity titanium sheets by constrained groove pressing. Materials science forum. 683:233–42.

[13] Thirugnanam, A., Kumar, T.S. and Chakkingal, U. 2010 Tailoring the bioactivity of commercially pure titanium by grain refinement using groove pressing. Mater Sci Eng C. 3(1):203–8.

[14] Peng, K., Su, L., Shaw, L.L. and Qian, KW. 2007. Grain refinement and crack prevention in constrained groove pressing of two-phase Cu-Zn alloys. Scrip Mater. 56(11):987–90.

[15] Meyers, MA., Mishra, A. and Benson, DJ. 2006. Mechanical properties of nanocrystalline materials. Prog Mater Sci. 51(4):427–556.

[16] Yoon, SC., Krishnaiah, A., Chakkingal, U. and Kim, HS. 2008. Severe plastic deformation and strain localization in groove pressing. Comput Mater Sci. 43:641–5.

[17] Hosseini, E. and Kazeminezhad, M. 2010. Integration of physically based models into FE analysis: Homogeneity of copper sheets under large plastic deformations. Comput Mater Sci. 48:166–73. doi:10.1016/j.commatsci.2009.12.023.

[18] Dhiliban, Chakravarthy and Kumar, A. 2024. Effect of Die Profile on Strain Inhomogeneity During Constrained Groove Pressing. Trans Indian Inst Met. 77:1787–1794. doi:10.1007/s126 66-023-03196-6.

[19] Zimina, M., Bohlen, J., Letzig, D., Kurz, G., Cieslar1, M. and Zrník, J. 2014. The study of microstructure and mechanical properties of twin-roll cast AZ31 magnesium alloy after constrained groove pressing. Materials Science and Engineering 63. doi:10.1088/1757-899X/ 63/1/012078.

[20] Nagarajua, K.N., Sunila, A.R., Sachina, K., Sujaya, H., S Siddeshaa, H. and Kumar, S. A. 2018. Influence of Constrained Groove Pressing Passes and Annealing Characteristics on the Mechanical Properties of 6061 Aluminum Alloy. Materials Today: Proceedings. 5:2660–2665. doi:10.1016 /j.matpr.2018.01.046.

[21] Mozafari, J., Khodabakhshi, F., Eskandari, H. and Haghshenas, M. 2019. Wear Resistance and Tribological Features of Ultra-FineGrained Al-Mg Alloys Processed by Constrained Groove Pressing-Cross Route. Journal of Materials Engineering and Performance. doi:10.1 007/s11665-019-3859-3.

[22] Nazari, F., Honarpisheh, M. and Zhao, H. 2019. Effect of stress relief annealing on microstructure, mechanical properties, and residual stress of a copper sheet in the constrained groove pressing process. The International Journal of Advanced Manufacturing Technology. 102:4361–4370. doi:10.1007/s00170-019-03511-w.

[23] Kumar, S., and Vedrtnam, A. 2021. Experimental and numerical study on effect of constrained groove pressing on mechanical behaviour and morphology of aluminium and copper.Journal of Manufacturing Processes. 67:478–486. doi:10.1016/j.jmapro.2021 .05 .008.

[24] Hosseini Faregh, S. S., Raiszadeh, R. and Dashtbayazi, M. R. 2024. Pure Copper Sheets Processed by Constrained Studded Pressing: The Effect of Die Angle. Journal of Materials Engineering and Performance. 33:3262–3272. doi:10.1007/s11665-023-08222-8.

[25] Wang, Z.S., Guan, Y.J. and Zhong, C.K. 2014. Effects of Friction on Constrained Groove Pressing of Pure Al Sheets. Advanced Materials Research. 926: 81-84.

[26] Adel, T., Abbas, A., Abubakr, M., Hassan, M.A., Luqman, M., Soliman M.S. and Hegab, H. 2020. An adaptive design for cost, quality and productivity-oriented sustainable machining of stainless steel 316. Journal of Materials Research and Technology. 9(6):14568-1458.

[27] Moslemi, N., Norizah, R., Norhayati, A. and Tang Nan, H. 2015. Effect of Current on Characteristic for 316 Stainless Steel Welded Joint Including Microstructure and Mechanical Properties. Procedia CIRP. 26:560 – 564. doi:10.1016/j.procir.2015.01.010.

[28] Kurgan, N. and Varol, R. 2010. Mechanical properties of P/M 316L stainless steel materials. Powder Technology.201(3):242-247. doi:1 0.1016/j.po wtec.2010.03.041.

[29] Solomon, N., and Solomon, I. 2010. Deformation induced martensite in AISI 316 stainless steel. revista de metalurgia. 46(2)121-128. doi: 10.3989/revmetalm. 0920.

[30] Maranhão, C. and Davim, J.P. 2010. Finite element modelling of machining of AISI 316 steel: Numerical simulation and experimental validation. Simulation Modelling Practice and Theory. 18(2):139-156.

[31] Lai, J.K.L. 1983. A study of precipitation in AISI type 316 stainless steel. Materials Science and Engineering. 58(2):195-209. doi:10.1016/0025-5416(83) 90046-0.

[32] Lee, J., Lee, C. and Kim, B. 2009. Reverse analysis of nano-indentation using different representative strains and residual indentation profiles. Materials and Design. 30:3395–3404. doi:10.1016/j .matdes.2009.03.030.

[33] Zheng, Y., Li, J., Tam, A.Y.C., Lee, T.T.Y., Peng, Y., Chung-Wai Cheung, J., Wai-Chi Wong, D. and Ni, M. 2025. Finite element modeling of clavicle fracture fixations: a systematic scoping review. Med Biol Eng Comput. 03294-1. doi: 10.1007/s11517-025-03294-1.

[34] Cadet, G. and Paredes, M. 2024. Convergence analysis and mesh optimization of finite element analysis related to helical springs. Mechanics & Industry. 25(22):20. doi:10.1051 /meca/2024018.